AIP | Applied Physics Letters

Electroacoustic properties of 110-oriented Pb(Mg 1/3 Nb 2/3) O 3 – PbTiO 3 crystals under uniaxial stress

D. Viehland, J. F. Li, K. Gittings, and A. Amin

Citation: Applied Physics Letters **83**, 132 (2003); doi: 10.1063/1.1591240
View online: http://dx.doi.org/10.1063/1.1591240
View Table of Contents: http://scitation.aip.org/content/aip/journal/apl/83/1?ver=pdfcov
Published by the AIP Publishing

Electroacoustic properties of ⟨110⟩-oriented $Pb(Mg_{1/3}Nb_{2/3})O_3-PbTiO_3$ crystals under uniaxial stress

D. Viehland[a] and J. F. Li
Department of Materials Science and Engineering, Virginia Tech, Blacksburg, Virginia 24061

K. Gittings and A. Amin
Naval Seacommand, Newport, Rhode Island 02841

(Received 13 February 2003; accepted 13 May 2003)

The electromechanical properties of ⟨110⟩-oriented $0.7Pb(Mg_{1/3}Nb_{2/3})O_3-0.3PbTiO_3$ crystals have been investigated under uniaxial stress (σ). ⟨110⟩-oriented crystals have a longitudinal electromechanical coupling coefficient (k_{33}) of ~0.9 and an acoustic power density of 12 dB which decreases to 8 dB with increasing σ between 0 and 4×10^7 N/m^2. The results demonstrate that the advantages in terms of power density and coupling coefficient of oriented piezocrystals are not constrained to the ⟨001⟩-orientation, but rather can also be obtained along the ⟨110⟩. © *2003 American Institute of Physics.* [DOI: 10.1063/1.1591240]

Single crystals of $(1-x)Pb(Mg_{1/3}Nb_{2/3})O_3-(x)PbTiO_3$ (PMN–x%PT) and $Pb(Zn_{1/3}Nb_{2/3})O_3-PbTiO_3$ (PZN–x%PT) are currently under development for use in transducer and projector applications.[1,2] Previous investigations have focused on ⟨001⟩-oriented crystals, for compositions in the ferroelectric rhombohedral phase (FE_r) ($x<30$ at. %), close to the morphotropic phase boundary. In poled ⟨001⟩-oriented single crystals, longitudinal piezoelectric (d_{33}) and electromechanical coupling (k_{33}) coefficients of 1800 pC/N and 0.94 have been reported,[1,2] respectively. Strain levels of up to 1.2% were reported at field levels of ~30 kV/cm. The potential advantages of ⟨001⟩-oriented PMN–PT crystals in transducer applications are twofold. First, the crystals have the potential for higher bandwidth due to an enhanced electromechanical coupling coefficient. Second, the crystals have the potential for higher projected acoustical energy density due to their higher strain. Acoustic power densities of ~12 dB have recently been obtained for ⟨001⟩-oriented specimens, under prestress.[3,4]

Recent investigations have shown high electromechanical coefficients for ⟨110⟩-oriented PMN–PT crystals.[5,6] Values of d_{33} and k_{33} were found to be equally high as those along the ⟨001⟩. An unusual electromechanical and elastic equivalence was found between the ⟨110⟩ and ⟨001⟩ directions. These investigations clearly demonstrated that the potential advantages of PMN–PT crystals for transducer applications are not constrained to a single crystallographic orientation, but rather to the (011) plane.

The purpose of this investigation was to study the effects of uniaxial stress on ⟨110⟩-oriented single crystals of $Pb(Mg_{1/3}Nb_{2/3})O_3-30\%PbTiO_3$. In acoustic transducer applications,[7,8] uniaxial prestress inherently needs to be used, in order to keep the transducer from going into tension and consequently to be able to harness the highest electromechanical response. Investigations have been performed using polarization versus field ($P-E$), strain versus field ($\varepsilon-E$), and strain versus stress ($\varepsilon-\sigma$) methods.

[a]Electronic mail: viehland@mse.vt.edu

⟨110⟩-oriented $Pb(Mg_{1/3}Nb_{2/3})O_3-30\%PbTiO_3$ grown by seeded vertical Bridgman methods[9–11] have been obtained from HC Materials (Urbana, IL). Plate-like specimens were cut into dimensions of ~0.4 cm×0.4 cm×0.04 cm, and bar-like specimens were cut into dimensions of ~0.4 cm×0.4 cm×1.2 cm. All specimens were electroded with gold. The specimens were poled at room temperature in a silicon oil bath, using a current-limiting method to prevent breakdown. $P-E$ measurements were made using a modified Sawyer–Tower bridge. In addition, $\varepsilon-E$ measurements were simultaneously performed using a strain gauge (bar-shaped specimens) or a LVDT method (plate-like specimens). For the bar-shaped specimens, strain gauges were mounted on the side of the bars and a mechanical load was applied using a pneumatic cylinder. These measurements were performed using a drive frequency of 10 Hz at maximum applied field strengths of 15 kV/cm. Measurements were performed as a function of mechanical prestress between 0 and 6×10^7 N/m^2.

Figures 1(a) and 1(b) show the unipolar $P-E$ and $\varepsilon-E$ characteristics for the plate-like specimens. These data are pronouncedly anhysteretic, over the entire range of E investigated all the way to saturation. In particular, the integrated area of the hysteresis loop in the $P-E$ response was nearly zero, at least within the limits of instrumentation error. Data are shown for three different maximum ac electric fields of 10, 20, and 40 kV/cm. The data demonstrate an induced phase transformation near 10 kV/cm, reaching saturation near 12 kV/cm. It is important to notice that this induced phase transformation was also anhysteretic. The magnitude of ΔP and ε at 12 kV/cm was 0.07 C/m^2 and 3×10^{-3}, respectively, which is a relatively high induced strain for a small ΔP. Accordingly, the piezoelectric (d_{33}) and electromechanical coupling (k_{33}) coefficients are high along the ⟨110⟩. Resonance-antiresonance investigations of ⟨110⟩-oriented PMN–PT crystals demonstrated equally high values of d_{33} (1500 pC/N) and k_{33} (0.94) coefficients. This dismisses the notion that the high electromechanical performance can only be due to an induced FE_t phase and/or po-

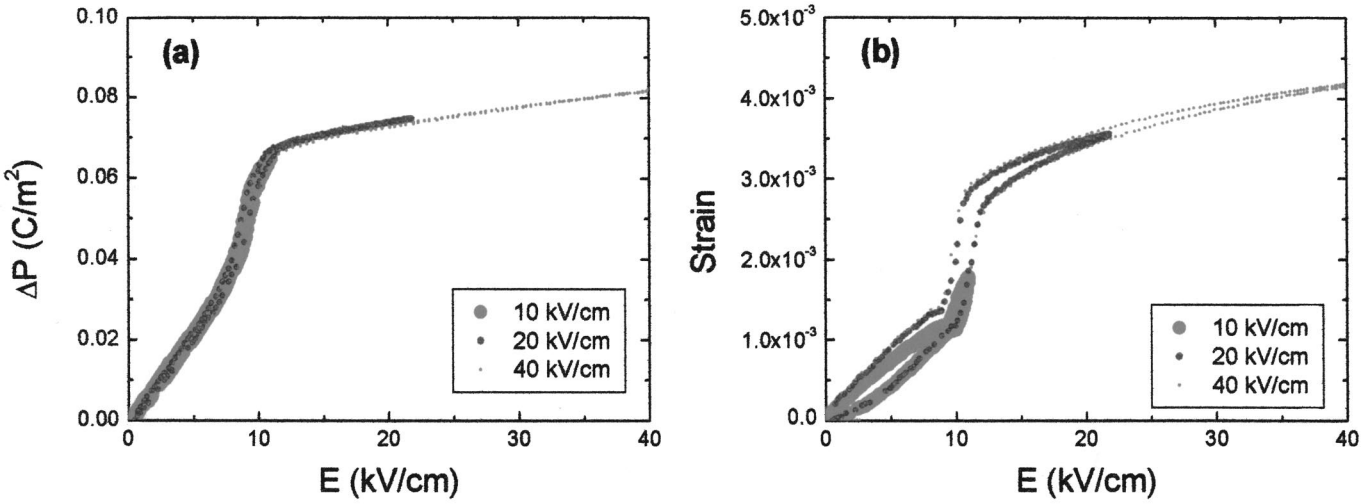

FIG. 1. Unipolar $P-E$ and $\varepsilon-E$ characteristics of ⟨110⟩-oriented PMN–PT plate-like crystals. (a) $P-E$ response, and (b) $\varepsilon-E$ response. Data are shown for various maximum ac drives of 10, 20, and 40 kV/cm. The data for the various maximum ac drives are distinguished by the size of the points in the figure.

larization rotation towards ⟨001⟩. In addition, the value of Young's modulus Y_1 was measured calculated to be 1.8×10^{10} N/m^2 from the standard resonance-antiresonance IEEE method.

Figures 2(a) and 2(b) show the unipolar $\Delta P-E$ and $\varepsilon-E$ responses for a bar-shaped ⟨110⟩-oriented crystal under various uniaxial stresses. Decreases in ΔP and ε are noticeable with increasing σ, in particular for $E>10$ kV/cm where the induced phase transition occurred. At $E=15$ kV/cm, ΔP decreased from ~0.07 C/m^2 under small loads to ~0.058 C/m^2 under 6×10^7 N/m^2. Correspondingly, ε decreased from $\sim1.9\times10^{-3}$ to $\sim1.4\times10^{-3}$ with increasing σ. The data reveal essentially no change in the hysteretic losses with increasing σ. The dominant change with increasing σ was to suppress the induced phase transformation, resulting in the $\Delta P-E$ and $\varepsilon-E$ responses becoming increasingly linear with increasing σ. For $\sigma=6\times10^7$ N/m^2, the electromechanical behavior is nearly ideally linear and anhysteretic, with an effective d_{33} of ~1000 pC/N, as determined from the slope. These results are in contrast to the stress-dependent electromechanical properties of ⟨001⟩-oriented crystals, which become increasingly nonlinear and hysteretic with increasing σ.[3,4] It is also important to note that there was a difference in the field level at which the step in strain occurred between the plate-like specimen of Fig. 1(b) (10 kV/cm), and the long-rectangular one of Fig. 2(b) (12 kV/cm). The differences are attributed to small composition variations that shift the critical field of the induced transition.

The electromechanical coupling coefficient (k_{33}) at various uniaxial loads can be calculated,[7,8] as given in Eq. (1):

$$k_{33}^2=d_{33}^2Y_1/(\chi_0K), \tag{1}$$

where Y_1 is Young's modulus, χ_0 is the permittivity of free space (8.85×10^{-12} F/m), K is the relative dielectric constant, and d_{33} is the longitudinal piezoelectric coefficient. K can be approximated from the $P-E$ response over a quasilinear range as $\delta P_3/\delta E_3$, and d_{33} can be approximated over a quasilinear range as $\delta\epsilon_3/\delta E_3$, both of which have limitations. Quasilinear approximations were performed for an E_{dc} of 8 kV/cm and an E_{ac} of 4 kV/cm. The value of Y_1 can be

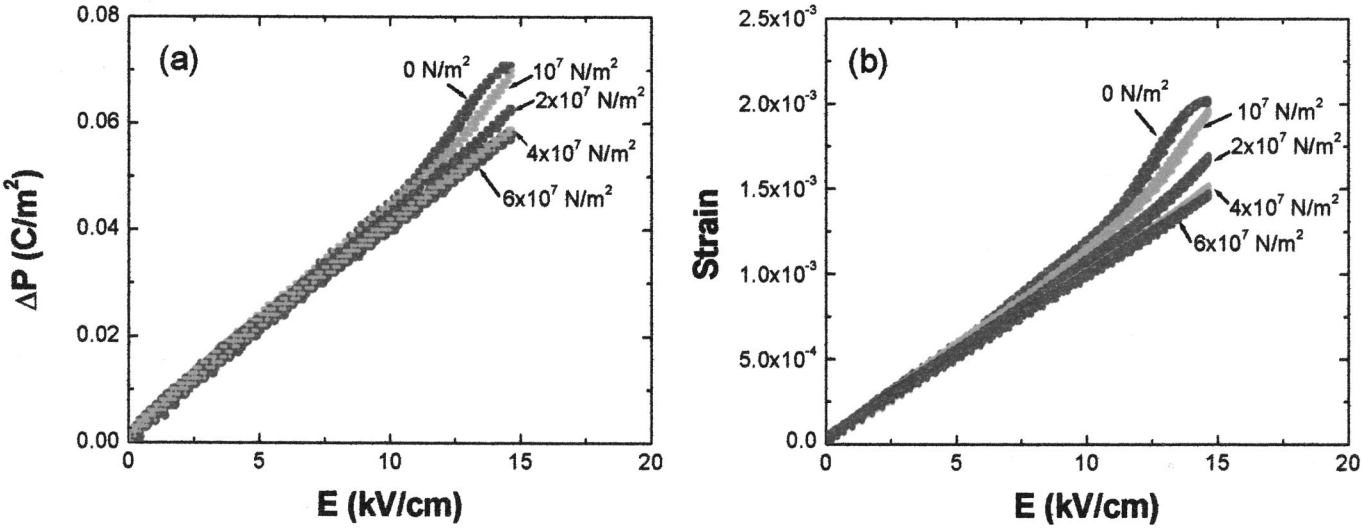

FIG. 2. $P-E$ and $\varepsilon-E$ responses for ⟨110⟩-oriented long-rectangular shaped crystals, taken at various uniaxial stresses between 0 and 6×10^7 N/m^2. (a) $P-E$ response, and (b) $\varepsilon-E$ response.

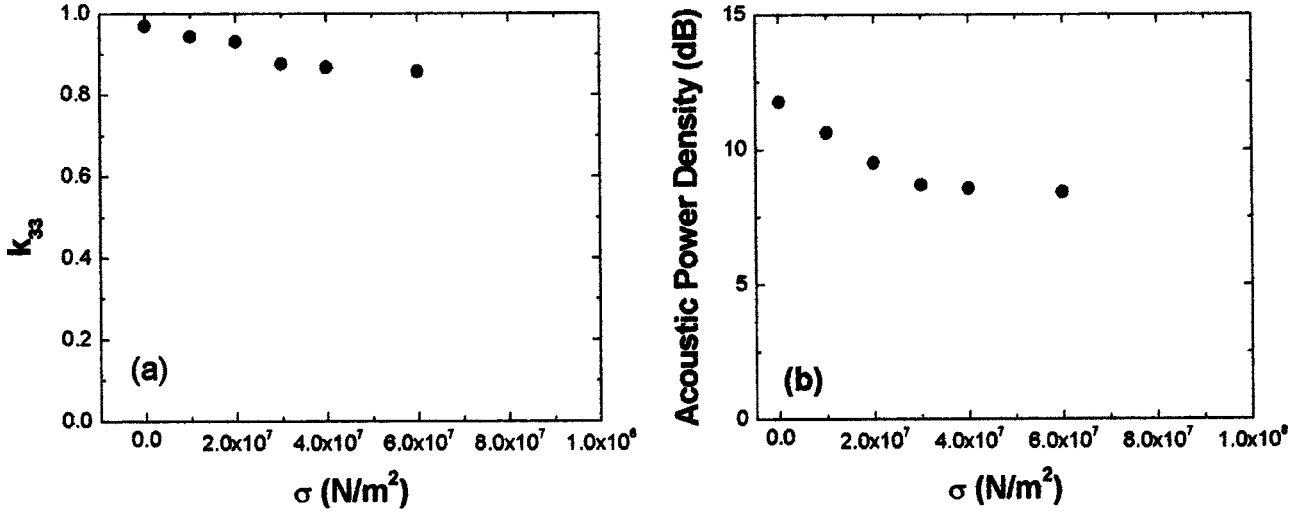

FIG. 3. Coupling coefficient and acoustic power density of ⟨110⟩-oriented PMN–PT long-rectangular crystals as a function of stress. (a) Coupling coefficient and (b) acoustic power density.

determined from measurements of the $\varepsilon-\sigma$ response. Accordingly, Y_1 was determined at various dc bias levels (E_{dc}) by stress-strain ($\varepsilon-\sigma$) measurements. The $\varepsilon-\sigma$ curves were linear and Y_1 was calculated from the slopes. The value of k_{33} is shown in Fig. 3(a) as a function of σ. In this figure, k_{33} can be seen to be somewhat independent of σ. For example, k_{33} varied between 0.95 at $\sigma=0$ N/m^2 to ~0.86 at $\sigma=6\times10^7$ N/m^2. The value of k_{33} under zero uniaxial stress is close to that determined by the resonance-antiresonance method earlier. These results clearly demonstrate ⟨110⟩-oriented crystals maintain a high electromechanical coupling coefficient under realistic operational conditions for use in acoustic transducers. In fact, k_{33} is equally as high along the ⟨110⟩, as along the ⟨001⟩.[1–4] This is essential to their use in high performance applications that require enhanced bandwidth.

By convention, the acoustical energy density can be defined relative to that of a standard PZT-8 material, as given in Eq. (2a);[7,8] where

$$\text{acoustic energy density(dB)} = 10\log(E_{\mathrm{elastic}}/E_{\mathrm{PZT\text{-}8}}), \tag{2a}$$

$$E_{\mathrm{elastic}} = 1/2 Y_1 \varepsilon_{\mathrm{rms}}^2. \tag{2b}$$

$E_{\mathrm{PZT\text{-}8}}$ is the acoustical energy density of the standard PZT-8. $E_{\mathrm{PZT\text{-}8}}$ is calculated by assuming a linear piezoelectric response over the operational field range, i.e., $\varepsilon_{ij}=d_{ijk}E_k$. The accepted values of d_{ijk} and Y_1 for PZT-8 are equal to 2.25×10^{-10} C/N and 7.4×10^{10} N/m^2. Thus, the value of $E_{\mathrm{PZT\text{-}8}}$ can be estimated as 936.6 J/m^3 under an applied electric field of 10 kV/cm. Using the values for E_{elastic}, the corresponding acoustical energy density can be calculated using Eq. (2a). Figure 3(b) shows the acoustical power density (dB) as a function of σ. In this figure, the acoustical power density can be seen to decrease with some with increasing σ. For example, the acoustic power density varied between 11.75 dB at $\sigma=0$ to ~9.5 dB at $\sigma=6\times10^7$ N/m^2.

The results demonstrate that ⟨110⟩-oriented PMN–PT crystals are near linear electromechanical materials with high acoustic energy densities, high coupling, and essentially no loss. For $\sigma<2\times10^7$ N/m^2, they offer a $k_{33}>0.95$ and an acoustic power density of ~10 dB. We believe that ⟨110⟩-oriented crystals have a unique character, which offers promise for transducer applications, even potentially over that of ⟨001⟩ crystals. This is that twinning occurs along the ⟨110⟩. A stress applied along the ⟨110⟩ will not favor one twin state over another. Thus, the electromechanical response has increased linearity and lower losses due to a lack of domain contributions, and better accommodation to applied stress.

The research was supported by the Office of Naval Research under Grant Nos. N000140210340, N000140210126, and MURI N000140110761.

[1] S. Park and T. R. Shrout, J. Appl. Phys. **82**, 1804 (1997).
[2] S. Park and T. R. Shrout, IEEE Trans. Ultrason. Ferroelectr. Freq. Control **44**, 1140 (1997).
[3] D. Viehland and J. Powers, J. Appl. Phys. **89**, 1820 (2001).
[4] D. Viehland, J. Powers, and J. F. Li, J. Appl. Phys. **90**, 2479 (2001).
[5] Y. Lu, Q. M. Zhang, and D. Viehland, Appl. Phys. Lett. **78**, 3109 (2001).
[6] D. Viehland, A. Amin, and J. F. Li, J. Appl. Phys. **92**, 3985 (2002).
[7] D. Stansfield, *Underwater Electroacoustic Transducers* (Bath University Press, Bath, United Kingdom, 1991).
[8] R. S. Wollett, J. Acoust. Soc. Am. **40**, 1112 (1966).
[9] W. Jiang, W. Cao, and P. Han, Appl. Phys. Lett. **80**, 2466 (2002).
[10] W. Tan, Z. Xu, J. Shang, and P. Han, Appl. Phys. Lett. **76**, 3732 (2000).
[11] M. Zhu and P. Han, Appl. Phys. Lett. **75**, 3868 (1999).